



## Preparation of Diamond/Ceramic Composite by Sol-Gel Method and Its Physical Properties

KAI GAO, ZHIHONG LI, LI NA, DONGDONG SHAN, KAIYUE WANG and YUMEI ZHU\*

<sup>1</sup>Key Laboratory of Advanced Ceramics and Machining Technology of Ministry of Education, School of Materials Science and Engineering, Tianjin University, Tianjin 300072, P.R. China

\*Corresponding author: Tel: +86 22 27406420; E-mail: kai781231@yahoo.com.cn

(Received: 31 October 2011;

Accepted: 8 September 2012)

AJC-12106

A diamond/ceramic composite was fabricated by sintering a composite precursor composed of a synthetic collosol and gelatine and thus the SiO<sub>2</sub>-Al<sub>2</sub>O<sub>3</sub>-B<sub>2</sub>O<sub>3</sub>-CaO-MgO-ZnO-K<sub>2</sub>O-Li<sub>2</sub>O ceramic phase was introduced into diamond powder. The gelatine powder was characterized with DSC, FTIR, SEM, EDS and XRD after thermal treatment. Results showed that the sol-gel method had dramatically reduced the softening temperature of the glass and the dose of the alkali metal added could be well-controlled. Meanwhile, the dielectric loss was ultimately reduced and the resistance and dielectric property of the sheet-shaped composite was calculated by means of a resonance circuit at high frequency. The results indicated that the resistance of diamond massive composite was slightly larger than that of diamond thin-film, while the dielectric loss of the former was less than 0.002 and lower than the latter.

**Key Words:** Sol-gel, Ceramic, Coating, Dielectric material, Diamond composite.

### INTRODUCTION

In recent years, with the rapid development of computer auxiliary equipment, mobile communications equipment and audio products, the demand for sheet-shaped inductance and the relevant component quantity is increasing year by year. Thus, the market favourably promotes the research and development of a relevant technique for producing such devices. With low permittivity and a thermal expansion coefficient which is compatible with silicon, diamond has enjoyed great application potential as a hyperthermia conductor and in electronic encapsulation<sup>1</sup>. Because of the relatively high price of the chemical vapour deposition (CVD) film and the great production capacity for making synthetic diamond<sup>2</sup>, the development of functional materials prepared with diamond micro-powder has become increasingly important<sup>3,4</sup>. Because of the physical properties of the film, such as its mechanics and thermology, can be enhanced by adjusting the content of each component in the ceramic phase, much interest and attention are being given to the diamond-reinforced ceramic-based (diamond/ceramic) composites<sup>5</sup>.

In the viscous flow mechanism during the sintering process of a composite, the liquid phase of the ceramic plays a crucial role. The activation energy of the sintering of the relevant material is calculated by means of formula 1:

$$\ln \left[ \frac{T_d \left( \frac{\Delta L}{L_0} \right)}{dT} \right] = \ln \left( \frac{1}{nK_0^{1/n}} \right) - \frac{1}{n} \ln \alpha - \frac{Q}{nRT} \quad (1)$$

where  $\Delta L/L_0$  is the linear contractibility, T is the thermodynamic temperature,  $\alpha$  is the set velocity, Q is the activation energy of sintering and R is the mol constant of the atmosphere.

It turns out that ceramic liquefaction serves as the velocity control of sintering<sup>6</sup>. Since diamond is easily oxidized at high temperature, a plentiful alkaline metal ion can be added to the ceramic phase to reduce the melting temperature. However, the content of the alkaline metal needs to be controlled since composites for electric packaging are required to have low dielectric constants and minimal dielectric losses, which is probably the reason there has been no discussion on the electrical or dielectrical properties of the specimens in relevant articles.

Sol-gel has become a valuable method for powder preparation in recent years. Its advantages include low in-process temperature, equal components of the product and a high degree of purity<sup>7,8</sup>. The preparation of a basic ceramic by means of the sol-gel method can avoid the conventional preparation method which requires a high-temperature melting-quenching

process and a further reduction of the sintering temperature. Therefore, a silica solution consisting of a  $\text{SiO}_2\text{-Al}_2\text{O}_3\text{-B}_2\text{O}_3\text{-CaO-MgO-ZnO-K}_2\text{O-Li}_2\text{O}$  ceramic phase was compounded in advance in this research. The sol was then added to the diamond powder to prepare the composite precursor to reduce the sintering temperature and obtain a diamond/ceramic composite with low dielectric constant and dielectric loss through a certain sintering system.

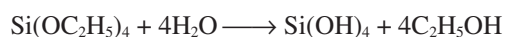
## EXPERIMENTAL

**Selection of the diamond grit:** By comparing the velocity of diamond-quality loss under different compounding conditions, previous workers have discovered that diamond grit whose particle size is on the order of micrometers is more suitable for compounding diamond composites and this recommendation has proven useful in many tasks<sup>4</sup>. Therefore, diamond powder (Henan Huajing Corporation) with a particle size of 40-50  $\mu\text{m}$  has been selected as the raw material for this experiment.

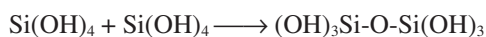
**Choosing each component of the formula:** Since the physical and chemical properties of crystalline diamond are very stable, research on the properties of a diamond composite is essentially a matter of choosing the proper ceramic phase components.  $\text{SiO}_2$ ,  $\text{Al}_2\text{O}_3$  and  $\text{B}_2\text{O}_3$  in the system serve as the frame structure. The alkaline-earth metal and alkaline metal act as the network modifier, with the two metals composing the glass phase of the ceramic phase, then forming the liquid phase during the sintering process of the composite and promoting the compacting of the composite<sup>9</sup>. The selection of each component of the formula in this study was based on research on the effect the amounts alkaline-earth metals and alkaline metals have on the formation of a ceramic-liquid phase and composite strength<sup>10</sup>, as well as on previous work conducted by the research team for this study.

**Preparation of precursor powder:** The process scheme is shown in **Scheme-I**. Tetraethyl orthosilicate (TEOS) and  $\text{C}_2\text{H}_5\text{OH}$  were mixed in certain proportions and vigorously stirred and then  $\text{H}_3\text{BO}_3$  in  $\text{C}_2\text{H}_5\text{OH}$  solution, the mixed aqueous solution of  $\text{Al}(\text{NO}_3)_3\text{-Ca}(\text{NO}_3)_2\text{-Mg}(\text{NO}_3)_2\text{-Zn}(\text{NO}_3)_2\text{-KNO}_3\text{-LiNO}_3$  was dropped into the TEOS solution (the mol proportions were  $\text{SiO}_2\text{:Al}_2\text{O}_3\text{:B}_2\text{O}_3\text{:CaO:MgO:ZnO:K}_2\text{O:Li}_2\text{O} = 0.419\text{:}0.03\text{:}0.10\text{:}0.183\text{:}(0.12-x)\text{:}0.11\text{:}0.02\text{:}x$ ). For convenience in calculating the added water, the mol weight of TEOS was set at the standard value of  $n\text{H}_2\text{O}/n\text{TEOS} = R$ , in which  $R = 30$  is defined in this experiment. With the hydrolyzing and condensation reactions in the solution, the sol was created when enough of a three-dimensional network of Si-O-Si in certain parts is formed. The main reactions in the process are as follows:

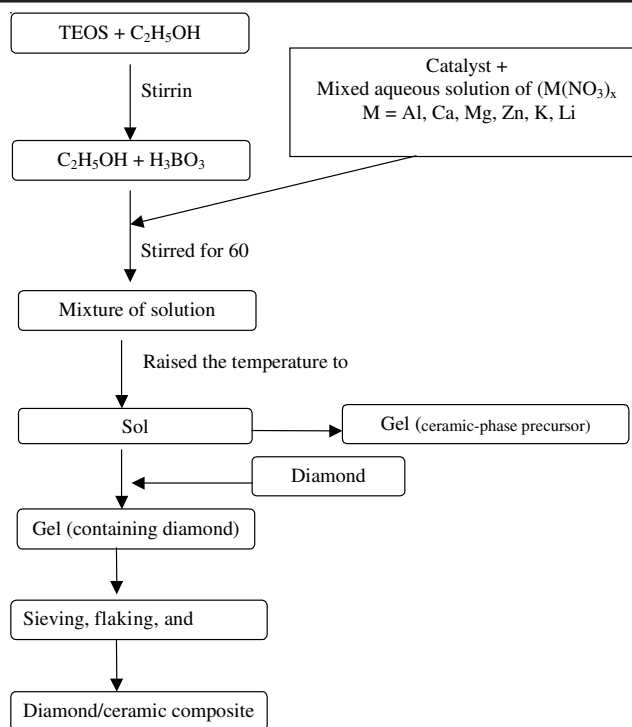
Hydrolyzing reaction:



Condensation reaction:



The sol was weighed with the proportion of ceramic and diamond powder (25:75). Sol and diamond powder of certain amount were mixed and maintained at a constant temperature of 343 K for 10 h. The ambient temperature was then raised to



**Scheme-I:** Flow chart for diamond/ceramic composite preparation by sol-gel processing

353 K after the formation of the gel and weighed every 0.5 h until the quality of the specimen remained constant and the precursor powder of the composite was then obtained.

Similarly, the residual sol without diamond powder was placed under constant temperature and the ambient temperature was raised to 353 K after the formation of the gel and weighed every 0.5 h until the quality of the specimen remained the same and the precursor powder of the ceramic phase was then obtained.

**Moulding and sintering of composite:** The precursor powder of the composite was compacted into a green sample  $\Phi 8 \times 1.5$  mm, which was put in a carborundum crucible with quartz sand covering it. The sample was then put into a resistance furnace at a velocity of 2 K/min and the temperature was raised to 1073 K and maintained at that temperature for 2 h. The specimen was taken out after it cooled to ambient temperature and ultrasonic-wave scrubbed by a mixture of  $\text{C}_2\text{H}_5\text{OH}$  and  $\text{CH}_3\text{COCH}_3$  (1:1) for 10 min and dried at 343 K.

**Analysis and representation:** Infrared spectrometer (NiColet-5DX-FT) was adopted to determine the molecular structural features of the gel powder both before and after the heat treatment and the composite mass, the setting was deducted twice and the precision was within  $2 \text{ cm}^{-1}$ . The thermal properties of the xerogel powder was analyzed by means of thermogravimetric-differential scanning calorimetry (TG-DSC, NETZSCH STA 449C, Germany), the resistance was measured by means of a ZC36 high-resistance meter and an impedance analyzer Agilent 4294A was used for the dielectric property test. The features and sizes of the grits were analyzed by an electric microscope PHLIPS XL30. The qualitative analysis of elements on the surface of the specimen after coating was analyzed by EDS. The model of XRD used was Rigaku D/Max 2500v/PC (1.54  $\text{\AA}$  ( $\text{CuK}_\alpha$  line)). The scanning angle

was from 10-90° and the velocity was 4°/min. X-Ray diffraction was used to analyze the phase structure.

The thermal conductivity of the specimen was measured by the heat flux method and the measuring instrument DRL-II (Hunan Xiangtan Instrument Co. Ltd.). The actual density of the specimen was measured by means of the Archimedes Principle. The thermal expansion coefficient was measured with a DIL402C (Netzsch Scientific Instruments Trading, Germany). The bar-type specimen was prepared according to the requirements and the bending strength of the specimen was measured by the three-point method.

## RESULTS AND DISCUSSION

**Analysis of DSC, FTIR and XRD of the ceramic-phase precursor powder:** Fig. 1 is the thermo-analysis curve of the ceramic-phase precursor powder after dehydration from room temperature to 1572 K. As seen from the DSC curve in Fig. 1, there are two heat-release peaks in the gel powder. The endothermic peak of 383 K corresponds to the residual water evaporation and decomposition of nitrate. The relatively wide heat-release peak of 558-873 K covers the decomposition of nitrate. The heat-release peak of 1018 K is the crystallization temperature  $T_c$ . The TG curve shows there was 55 % weight loss of the xerogel in the end and the weight loss ended at 873 K. Thus, the softening temperature was dramatically decreased by mean of the sol-gel method.

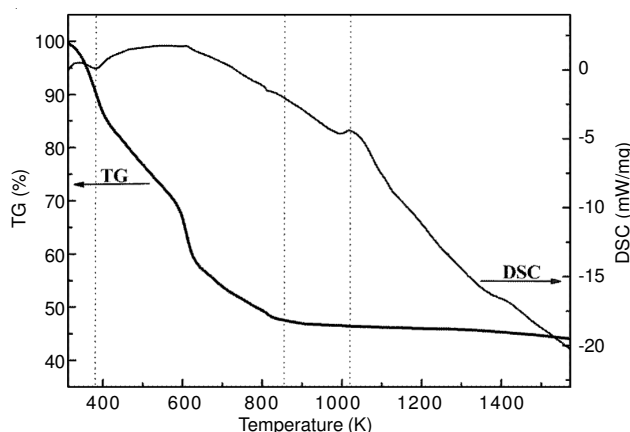


Fig. 1. Thermo-analysis curve of the ceramic-phase precursor powder after dehydration:  $x = 0.02$

Fig. 2 shows the XRD spectrum of the ceramic-phase precursor powder both before and after heat treatment. It indicates that the xerogel before heat treatment was an amorphous system without crystallization, with diopside precipitated from the ceramic phase after heat treatment. Diopside is a crystal of inosilicate<sup>11</sup> and it can ultimately form spherical silicate by adding additional water ( $R > 20$ ) under the condition of acid. However, the XRD spectrum also shows that the trend of creating inosilicate still played the dominating role under the experimental conditions. The formula of diopside in theory is composed of 55 %  $\text{SiO}_2$ , 25.9 %  $\text{CaO}$  and 18.5 %  $\text{MgO}$ . It therefore can be reckoned that the ratio of divalent to monovalent metal ion is 2.16:1 and the double alkali effect would greatly increase the resistivity of the composite. Meanwhile,  $\text{Al}^{3+}$  can take over the centre of the  $\text{AlO}_4$  tetrahedron

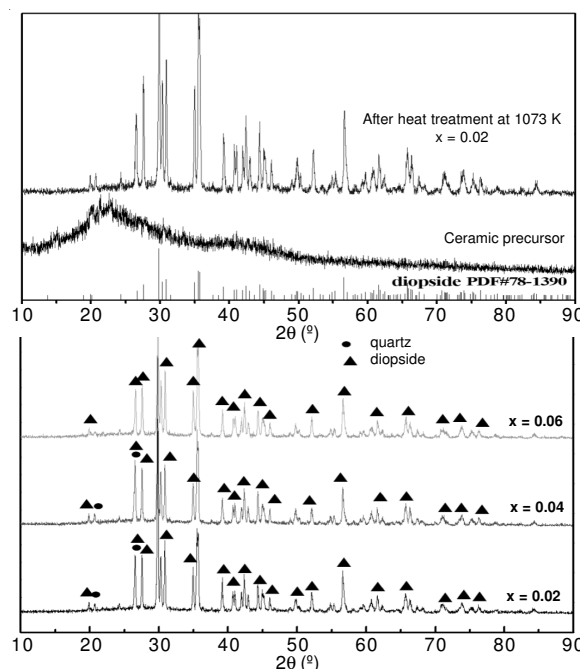


Fig. 2. XRD spectrum of the ceramic-phase precursor powder before and after heat treatment

and form the glass network, which would intensify the compactness of the network and further prevent the ions with weak ties from transference since the mol sum of alkaline earth metal and alkaline metal and  $\text{AlO}_4$  is greater than 1. With the increase of the ion content, the  $\text{SiO}_2$  precipitation of the ceramic phase was controlled and the formation of the ceramic phase was changed. The effect on the dielectric constants of the composite was then compared.

Fig. 3 shows the infrared spectrum of the xerogel before and after heat treatment. It can be seen that the peak of the  $\text{SiO}_4$  tetrahedron within the gel with vibration features disappears, indicating the polymerization reaction under 1073 K was accomplished. Since the compacting of the network was intensified, the bond absorption peaks of B-O, Si-O-Si and Si-O-B ( $1030$  and  $1083 \text{ cm}^{-1}$ ) were gradually broadened and combined<sup>12</sup>; the area near  $1384 \text{ cm}^{-1}$  is the absorption peak resulting from the contraction and vibration of the  $\text{NO}_3^-$  ion and the B-O bond. The absorption peak at  $1420 \text{ cm}^{-1}$  of curve B<sub>2</sub> is the new absorption peak resulting from the B-O tetrahedron under heat-treatment<sup>13</sup> rather than the deviation of the  $1384 \text{ cm}^{-1}$  absorption peak to a high-wave direction. The contraction and vibration peaks of the -C-H, -O-H, -C-O and -C=O bonds at  $3400$  and  $1640 \text{ cm}^{-1}$  disappeared because of organic decomposition. The absorption peak at  $485 \text{ cm}^{-1}$  resulted from the flexural vibration of -O-Si and Si-O-Al and the heat treatment had no obvious effect on the FTIR spectrum of this kind of vibration bond<sup>14</sup>.

**Analysis of FTIR and SEM of diamond/ceramic composite:** Fig. 4 shows the infrared spectrum of the diamond/ceramic composite at 1073 K for 2 h. It indicates that after the ceramic precursor was coated on the surface of diamond, the vibration peak of the -C-O and -C=O bonds ( $1720 \text{ cm}^{-1}$ ) recurred, in addition to those of the B-O tetrahedron ( $1350 \text{ cm}^{-1}$ ) and the Si-O-Si tetrahedron ( $972$  and  $860 \text{ cm}^{-1}$ , respectively). Because the reaction on the surface of diamond

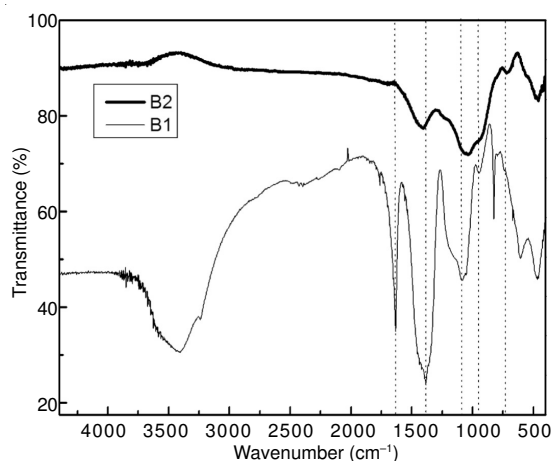


Fig. 3. Infrared spectrum of the xerogel ( $x = 0.02$ ) before heat treatment (B<sub>1</sub>) and after (B<sub>2</sub>) heat treatment

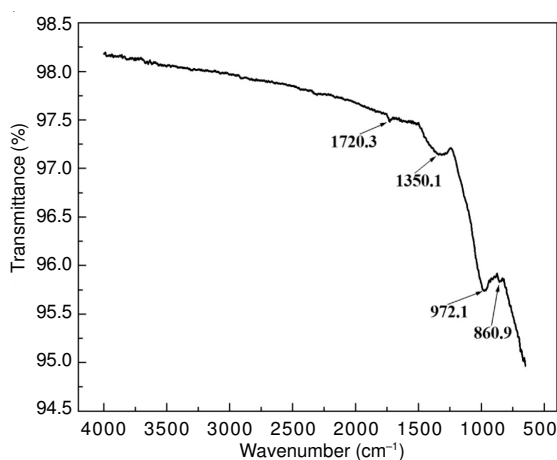


Fig. 4. Analysis of FTIR of diamond/ceramic composite:  $x = 0.02$

$C_{\text{diamond}} + M_xO_y \rightarrow xCO + yM^{15}$ ,  $M_xO_y$  can represent  $R_2O$ ,  $B_2O_3$ ,  $SiO_2$ , or  $ZnO$ . The research team once discussed the advantageous effects of  $ZnO$  on the interface reaction of ceramic and diamond, which was also the reason for the addition of a certain amount of  $ZnO$  in the formula<sup>16</sup>.

After the precursor of the diamond/ceramic composite was preserved at 1073 K for 2 h, there were no distinct crystal faces or angle edges (Fig. 5(b-1), 5(b-2), 5(b-3)) and there were no distinct cracks or pores in the polycrystalline films on the surface. EDS (the curve in (c)) in the square area shows that there are elements K and Zn in the film, in addition to Si, Al, Ca, Mg and O diopside. The analysis indicated that the polycrystalline film was coated on the diamond surface, even though the thickness of the film was not even, as seen from Fig. 5(b-1). Seen from Fig. 5(d-f), the specimen was a typical multiphase system, *i.e.*, including crystallized phases (diamond and diopside), glass phases and a small number of pore phases.

**Dielectric constants and dielectric losses of the diamond/ceramic composite:** Dielectric constants and dielectric losses of the sheet-shape composite were measured by a resonance circuit, with the results shown in Fig. 6. It can be seen that the dielectric loss of a single specimen gradually declined with an increase in frequency, meaning that the loss mechanism that existed within the frequency range of the diamond composite may have resulted from both the structure loss and the

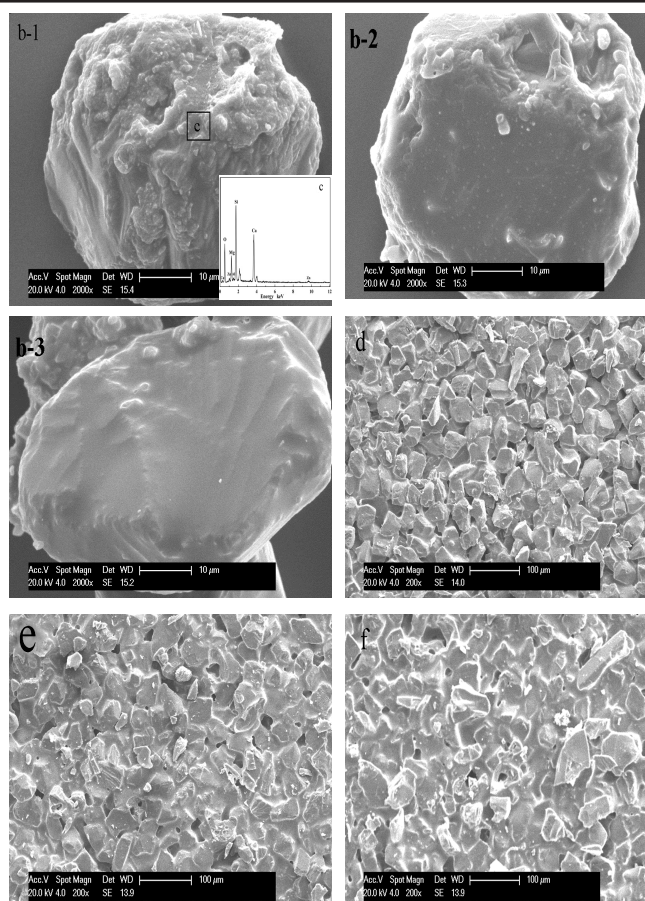


Fig. 5. (b) is the diamond/ceramic crystal (5(b-1):  $x = 0.02$ , 5(b-2):  $x = 0.04$ , 5(b-3):  $x = 0.06$ ) after heat preservation at 1073 K for 2 h, Fig. 5(d-f) is the cross-section of the diamond/ceramic composite. (d):  $x = 0.02$ , (e):  $x = 0.04$ , (f):  $x = 0.06$

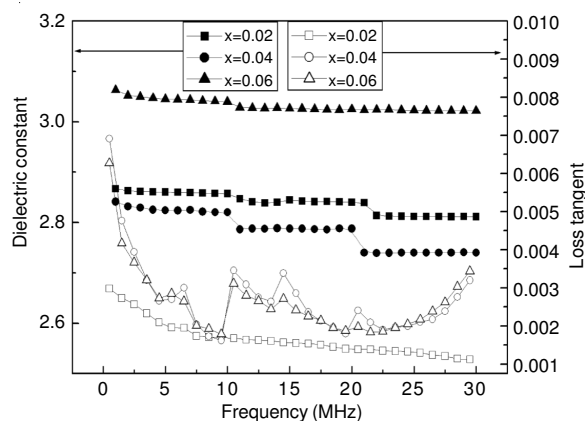


Fig. 6. Dielectric constants and dielectric losses of the sheet-shape composite at the range of 1-30 MHz

conductance loss. The structure loss was closely related to the compactness of the internal structure of the material. The increase of  $Li^+$  may have destroyed the lattice structure of the glass and the decline of the compactness may have led to the increase in dielectric loss. The more alkaline metal ions there are, the more compact the glass structure will be and the greater the possibility of a deviation of ions and of more structure loss. However, there was no relation between thermogravimetric analysis in the structure loss and frequency. The alkaline metal ions residing in the glass phase form a bond with the

TABLE-1  
COMPARISON OF DIELECTRIC PROPERTIES PARAMETERS OF  
DIAMOND SHEET-SHAPE COMPOSITE AND ALL THE DIAMOND FILMS

	Conventional diamond films <sup>18</sup>	Diamond-like carbon films <sup>19</sup>	Nanocrystalline diamond films <sup>20</sup>	Composite diamond/ceramic (x = 0.02)
Resistivity ( $\Omega$ cm)	$10^{13}$ - $10^{14}$	–	$> 10^{13}$	$> 10^{15}$
Dielectric constants	6.63-11.05	1.5	–	2.92 (1 MHz)
Dielectric losses	0.009-0.051 (1 MHz)	–	0.002 (10 MHz)	0.0027 (1 MHz) 0.0015 (10 MHz)

TABLE-2  
COMPARISON OF THE MECHANICAL PROPERTIES AND THERMAL PROPERTIES OF DIAMOND COMPOSITE

	Actual density ( $\text{kg m}^{-3}$ )	Coefficient of thermal expansion ( $300\text{-}823\text{ K}) \times 10^{-6} \text{ K}^{-1}$	Thermal conductivity ( $\text{W m}^{-1} \text{ K}^{-1}$ )	Bond strength (MPa)
x = 0.02	2.131	3.58	12.9	89
x = 0.04	2.145	3.55	12.1	91
x = 0.06	2.149	3.56	12.8	90

two  $\text{O}^{2-}$  to extend the lattice network, which makes for weak ties between the ions. There may be electrode penetration under the impact of an outer electric field and conductance loss. The more weakly tied ions there are, the greater the conductance loss. The conductance loss is featured with the decline of thermogravimetric analysis with the increase of frequency.

Since the structure of the composite is complicated, it was difficult to interpret the dielectric constant measured by means of an empirical mould. However, the small amount of pores in the specimen was undoubtedly one of the reasons for the decline of a valid dielectric constant<sup>17</sup>.

Table-1 shows the comparison of the dielectric properties of the diamond sheet-shape composite and all the diamond films. It indicates that the resistivity of the diamond composite was relatively larger than that of the diamond film. The dielectric loss in the literature<sup>20</sup> is given as 10 MHz. The minimum dielectric loss of the diamond composite in our study was less than 0.002 and  $\text{tg}\alpha$  was less than that of the nanometre-scale diamond film.

Table-2 shows the testing results of mechanical properties and thermal properties of the specimen. As can be seen from the table, the coefficients of thermal expansion are extremely approximate to those of silicon and the cracking caused by a mismatch between thermal expansion coefficients of different materials should be avoided in practice. The increase of  $\text{Li}^+$  rarely has an effect on the thermal properties of the composite. The thermal conductivity of the composite is relatively lower than that of diamond, significantly higher than that of glass ceramic and close to that of  $\text{Al}_2\text{O}_3$ . Tables 1 and 2 show that the amount of alkaline metal has the greatest effect on the dielectric properties of the composite and the least effect on the thermal properties during the preparation of the diamond ceramic composite.

## Conclusion

A ceramic phase precursor was combined with diamond by way of coating by the sol-gel method. The diamond phase (diamond and diopside) was obtained by sintering, creating a diamond-ceramic composite with glass phases as well some pore phases. The resistivity of the diamond composite was

relatively higher than that of diamond-alone film, while the dielectric loss was less. The sol-gel method greatly reduced the softening temperature and when the addition of the alkaline metal was controlled, diamond composites, whose dielectric properties were superior to those of diamond films, were eventually obtained. It is worth mentioning that the preparation method of the composite is simpler, making the mass manufacture of such composites possible.

## REFERENCES

1. M. Werner and R. Locher, *Reports Progress Phys.*, **61**, 1665 (1998).
2. Z.H. Li, P. Jia, L. Li, *Advanced Materials Research: Advances in Abrasive Technology XII*, pp. 76-78, 678 (2009).
3. T. Schubert, L. Ciupinski, W. Zielinski, A. Michalski, T. Weißgärber and B. Kieback, *Scripta Mater.*, **58**, 263 (2008).
4. E.A. Ekimov, N.V. Suetin, A.F. Popvich and V.G. Ralchenko, *Diamond Rel. Mater.*, **17**, 838 (2008).
5. X.H. Zhang, Y.H. Wang, J.B. Zang, J. Lu, J.H. Zhang and E.B. Ge, X.Z. Cheng, *Surf. Coat. Technol.*, **204**, 2846 (2010).
6. C.R. Chang and J.H. Jean, *Ceramic Trans.*, **97**, 227 (1999).
7. A.J. Zhang, Z.H. Li, Z.C. Li and Y.M. Zhu, *J. Sol-Gel Sci. Technol.*, **49**, 6 (2009).
8. F.H. Gong, Ch. Q. Liu and Q. Liu, *J. Chem. Ind. Eng. (China)*, **58**, 3197 (2007).
9. M. Jackson, N. Balow and B. Mills, *J. Mater. Sci. Lett.*, **13**, 1287 (1994).
10. Pengfei Wang, Zhihong Li and Yumei Zhu, *J. Non-Crystalline Solids*, **354**, 3019 (2008).
11. A. Duran, C. Serna and V. Fornes, *J. Non-Crystalline Solids*, **82**, 69 (1986).
12. H. Aguiar, J. Serra, P. González and B. León, *J. Non-Crystalline Solids*, **355**, 475 (2009).
13. B. Procyk, B. Stainewicz-Brodnik and K. Majewska-Albin, *Interceram.*, **49**, 308 (2000).
14. A.A. Egorov and M.A. Semin, *Glass Ceramics*, **64**, 190 (2007).
15. V.V. Solov'ev, V.V. Malyshev and A.I. Gab, *Theor. Found. Chem. Eng.*, **38**, 205 (2004).
16. P.F. Wang, Zh. H. Li, J. Li and Y.M. Zhu, *Solid State Sci.*, **11**, 1427 (2009).
17. H. Sakae, N. Yoshimura, S. Shingubara and T. Takahagi, *Appl. Phys. Lett.*, **83**, 2226 (2003).
18. H.W. Xin, Z.M. Zhang, X. Ling, Z.L. Xi, H.S. Shen, Y.B. Dai and Y.Z. Wan, *Diamond Rel. Mater.*, **11**, 228 (2002).
19. K.V. Ravi, US2008226841-A1; US7604834-B2 (2008).
20. M. Bevilacqua, N. Tumilty, A. Chaudhary, H. Ye, J.E. Butler and R.B. Jackman, *Diamond Electronics-Fundamentals To Applications II*, Materials Research Society, Boston (2008).